

COSMOPOWER-JAX: HIGH-DIMENSIONAL BAYESIAN INFERENCE  
WITH DIFFERENTIABLE COSMOLOGICAL EMULATORSD. PIRAS<sup>\*1</sup> AND A. SPURIO MANCINI<sup>†2</sup><sup>1</sup> Département de Physique Théorique, Université de Genève, 24 quai Ernest Ansermet, 1211 Genève 4, Switzerland and<sup>2</sup> Mullard Space Science Laboratory, University College London, Holmbury St. Mary, Dorking, Surrey, RH5 6NT, UK(Dated: 11th May 2023)  
submitted XXX; accepted YYY

## Abstract

We present **CosmoPower-JAX**, a JAX-based implementation of the **CosmoPower** framework, which accelerates cosmological inference by building neural emulators of cosmological power spectra. We show how, using the automatic differentiation, batch evaluation and just-in-time compilation features of JAX, and running the inference pipeline on graphics processing units (GPUs), parameter estimation can be accelerated by orders of magnitude with advanced gradient-based sampling techniques. These can be used to efficiently explore high-dimensional parameter spaces, such as those needed for the analysis of next-generation cosmological surveys. We showcase the accuracy and computational efficiency of **CosmoPower-JAX** on two simulated Stage IV configurations. We first consider a single survey performing a cosmic shear analysis totalling 37 model parameters. We validate the contours derived with **CosmoPower-JAX** and a Hamiltonian Monte Carlo sampler against those derived with a nested sampler and without emulators, obtaining a speed-up factor of  $\mathcal{O}(10^3)$ . We then consider a combination of three Stage IV surveys, each performing a joint cosmic shear and galaxy clustering (3x2pt) analysis, for a total of 157 model parameters. Even with such a high-dimensional parameter space, **CosmoPower-JAX** provides converged posterior contours in 3 days, as opposed to the estimated 6 years required by standard methods. **CosmoPower-JAX** is fully written in Python, and we make it publicly available to help the cosmological community meet the accuracy requirements set by next-generation surveys. 

## 1. INTRODUCTION

Bayesian inference of cosmological parameters from next-generation large-scale structure (LSS) and cosmic microwave background (CMB) surveys such as *Euclid* (Laureijs et al. 2011)<sup>1</sup>, the Vera Rubin Observatory (Ivezic et al. 2019)<sup>2</sup>, the Nancy Grace Roman Space Telescope (Spergel et al. 2015)<sup>3</sup>, the Simons Observatory (Ade et al. 2019)<sup>4</sup>, CMB-S4 (Abazajian et al. 2016)<sup>5</sup>, and CMB-HD (Sehgal et al. 2019)<sup>6</sup>, will require the exploration of high-dimensional parameter spaces –  $\mathcal{O}(100)$  parameters and higher – necessary to accurately model the physical signals and their several systematic contaminants. Sampling the posterior distribution in these high-dimensional spaces represents a significant computational challenge for Markov Chain Monte Carlo (MCMC) algorithms (Roberts et al. 1997; Katafygiotis & Zuev 2008; Liu 2009), which are traditionally used in cosmological analyses (Lewis & Bridle 2002; Audren et al. 2013; Brinckmann & Lesgourgues 2019; Torrado & Lewis 2021). Gradient-based inference methods, such as Hamiltonian Monte Carlo (HMC, Duane et al. 1987; Neal 1996) and variational inference (VI, Hoffman et al. 2013; Blei et al. 2017), manage to concentrate the sampling in regions of high posterior density, even in large para-

meter spaces, provided one has efficient access to accurate derivatives of the likelihood function with respect to the model parameters (Brooks et al. 2011; Neal 2011; Zhang et al. 2017; Betancourt 2017). Combining differentiable and computationally inexpensive likelihood functions with gradient-based inference techniques is thus crucial to efficiently obtain unbiased posterior distributions in high-dimensional parameter spaces.

Recently, there has been growing interest in the use of machine learning emulators to accelerate cosmological parameter estimation (e.g. Mootoovaloo et al. 2020; Arico et al. 2022; Nygaard et al. 2022; Günther et al. 2022). Spurio Mancini et al. (2022) (SM22 hereafter), in particular, developed **CosmoPower**, a suite of neural network emulators of cosmological power spectra that replaces the computation of these quantities traditionally performed with Einstein-Boltzmann solvers such as the Code for Anisotropies in the Microwave Background (CAMB, Lewis & Challinor 2011) or the Cosmic Linear Anisotropy Solving System (CLASS, Blas et al. 2011). In SM22 the authors show how Bayesian inference of cosmological parameters can be accelerated by several orders of magnitude using **CosmoPower**; the speed-up becomes particularly relevant when the emulators are employed within an inference pipeline that can be run on graphics processing units (GPUs).

An additional advantage in using machine learning emulators is that they efficiently provide accurate derivatives with respect to their input parameters. This is made possible by the *automatic differentiation* features implemented in the libraries routinely used to build these emulators, such as **TensorFlow** (Abadi et al. 2015), JAX

<sup>\*</sup> E-mail: davide.piras@unige.ch<sup>†</sup> E-mail: a.spuriomancini@ucl.ac.uk<sup>1</sup> <https://www.euclid-ec.org/><sup>2</sup> <https://www.lsst.org/><sup>3</sup> <https://roman.gsfc.nasa.gov/><sup>4</sup> <https://simonsobservatory.org/><sup>5</sup> <https://cmb-s4.org/><sup>6</sup> <https://cmb-hd.org/>

(Frostig et al. 2018) or PyTorch (Paszke et al. 2019). Automatic differentiation (*autodiff*, Bartholomew-Biggs et al. 2000; Neidinger 2010; Baydin et al. 2018; Paszke et al. 2017; Margossian 2019) can be used in gradient-based sampling algorithms to compute the derivatives of the likelihood function, provided the emulators are inserted within likelihood functions that can also be automatically differentiated. In practice, this means that the entire software implementation of the likelihoods should be written using primitives that belong to the aforementioned libraries. This is, for example, the main idea behind *jax-cosmo* (Campagne et al. 2023), a JAX-based library recently developed to compute cosmological observables, validated against the widely used Core Cosmology Library (CCL, Chisari et al. 2019). For other examples of gradient-based inference in cosmology, see e.g. Hajian (2007); Taylor et al. (2008); Jasche et al. (2010); Jasche & Wandelt (2013); Lavaux & Jasche (2015); Valade et al. (2022); Loureiro et al. (2023); Porqueres et al. (2023); Ruiz-Zapatero et al. (2023).

In this paper, we first develop an implementation of **CosmoPower** built using purely JAX primitives. We train the neural network emulators on the same data used in SM22, achieving an accuracy similar to that obtained by the TensorFlow-based implementation of SM22. We additionally compare the derivatives of the power spectra with respect to the input cosmological parameters computed using *autodiff* against those obtained with numerical differences and CAMB, showing a good agreement overall. We then couple **CosmoPower-JAX** with *jax-cosmo* to build likelihood functions completely written in JAX; this allows us to run parameter estimation pipelines using gradient-based algorithms on GPUs over very large parameter spaces. In particular, we consider two examples of future Stage IV survey configurations. In the first one, we study a single cosmic shear survey with typical Stage IV specifications; we compare the posterior contours obtained with our JAX-based pipeline against those obtained with a standard pipeline based on CCL, CAMB and the nested sampler *PolyChord* (Handley et al. 2015a,b). In the second case, we consider a joint analysis of three Stage IV surveys, each carrying out a joint shear - galaxy clustering (3x2pt) analysis. We show how **CosmoPower-JAX** enables efficient exploration of the 157-dimensional parameter space required for the modelling of the observables at a fraction of the time that would be required with traditional methods. In both experiments, inference is performed using the No U-Turn Sampler (NUTS) HMC variation (Hoffman & Gelman 2014), as implemented in the *NumPyro* library (Bingham et al. 2019; Phan et al. 2019).

The structure of this paper is as follows. In Sec. 2 we first describe our new JAX emulators and how they are trained on the same data used in SM22. We then review gradient-based methods for posterior inference and describe our JAX-based cosmological likelihoods. In Sec. 3 we validate the accuracy of our emulators and report our inference results in the two simulated Stage IV configurations described above. We conclude in Sec. 4. We make **CosmoPower-JAX**, which is fully written in Python, publicly available.<sup>7</sup>

<sup>7</sup> <https://github.com/dpiras/cosmopower-jax>

## 2. METHODS

### 2.1. **CosmoPower-JAX**

**CosmoPower** is a suite of neural network emulators of cosmological power spectra, namely matter and cosmic microwave background power spectra (albeit the emulation framework is highly flexible and can be used to emulate any other cosmological quantity; see e.g. Burger et al. 2023; Gong et al. 2023). Power spectra represent the key component of 2-point statistics analysis of cosmological fields, and are typically computed by Einstein-Boltzmann solvers such as CAMB or CLASS. These computations usually represent the main bottleneck in parameter estimation pipelines, particularly when high accuracy is required or when the cosmological scenario considered is not standard (see e.g. Spurio Mancini & Pourtisidou 2022; Balkenhol et al. 2022; Bolliet et al. 2023).

**CosmoPower-JAX** is a JAX-based implementation of **CosmoPower**; as such, it implements the same two emulation methods present in the original **CosmoPower** software. These are either a direct neural network mapping between cosmological parameters and logarithmic spectra, or a neural network mapping between cosmological parameters and the coefficients of a principal component analysis (PCA) of the spectra; we refer to SM22 for a detailed discussion. In our release version of **CosmoPower-JAX** these differences are dealt with internally; therefore, the user can simply obtain fast predictions of cosmological power spectra in three lines of code.

The neural networks we employ are made of four layers of 512 nodes each, with the same activation function described in SM22. In the case of the CMB temperature-polarisation and lensing power spectra, we preprocess the spectra using PCA, keeping 512 and 64 components, respectively. We optimise the mean-squared-error loss function using Adam (Kingma & Ba 2015), and keep a constant batch size of 512. The starting learning rate is  $10^{-2}$ , which we decrease by a factor of 10 (until  $10^{-6}$ ) every time the validation loss does not improve for more than 40 consecutive epochs.

Building the emulators in JAX unlocks its automatic-differentiation features, as well as the efficient batch evaluation and just-in-time compilation. Importantly, JAX is built around the popular NumPy library (Harris et al. 2020), which facilitates its use and portability. We refer the reader to Frostig et al. (2018) and Campagne et al. (2023) for a complete description of the features of JAX, especially in the context of cosmological analyses.

### 2.2. *Data*

We consider the same datasets as in SM22 to train and validate our emulators. Using CAMB, we produce a total of  $\sim 2 \times 10^5$  matter power spectra at 420 wavenumbers in the interval  $k \in [10^{-5} - 10]$  Mpc $^{-1}$  and with varying redshift  $z \in [0, 5]$ . We consider both the linear matter power spectrum  $P_{\delta\delta}^L$  and the non-linear correction  $P_{\delta\delta}^{\text{NL-CORR}}$ , such that the non-linear matter power spectrum  $P_{\delta\delta}$  can be written as:

$$P_{\delta\delta}(k, z) = P_{\delta\delta}^L(k, z) P_{\delta\delta}^{\text{NL-CORR}}(k, z), \quad (1)$$

where  $P_{\delta\delta}^{\text{NL-CORR}}$  is computed with *HMcode* (Mead et al. 2015, 2016). This non-linear correction introduces two extra baryonic parameters: the minimum halo concen-

tration  $c_{\min}$ , and the halo bloating  $\eta_0$ , which we vary when performing Bayesian inference.

Using CAMB we also produce  $\sim 5 \times 10^5$  CMB power spectra, including the temperature  $C_\ell^{\text{TT}}$ , polarisation  $C_\ell^{\text{EE}}$ , temperature-polarisation  $C_\ell^{\text{TE}}$  and lensing potential  $C_\ell^{\phi\phi}$  power spectra in the interval  $\ell \in [2, 2508]$ . All emulators are trained on the same parameter range indicated in table 1 of SM22. In both cases, we use  $\sim 90\%$  of the data to train the neural networks (of which we leave 10% for validation), and evaluate the trained models on the remaining  $\mathcal{O}(10^4)$  test spectra.

### 2.3. Gradient-based Bayesian inference

The goal of Bayesian inference is to sample the posterior distribution  $p(\boldsymbol{\theta}|\mathbf{d})$  of some parameters  $\boldsymbol{\theta}$  given observed data  $\mathbf{d}$ . Bayes' theorem relates the posterior distribution to the likelihood function  $p(\mathbf{d}|\boldsymbol{\theta})$ :

$$p(\boldsymbol{\theta}|\mathbf{d}) = \frac{p(\mathbf{d}|\boldsymbol{\theta})p(\boldsymbol{\theta})}{p(\mathbf{d})}, \quad (2)$$

where  $p(\boldsymbol{\theta})$  expresses prior knowledge on the parameters  $\boldsymbol{\theta}$ , and the evidence  $p(\mathbf{d})$  is a normalisation factor commonly ignored in parameter estimation tasks.

Drawing from  $p(\boldsymbol{\theta}|\mathbf{d})$  requires the use of stochastic samplers to generate a list of samples drawn from the posterior distribution. MCMC and nested sampling algorithms are the two main classes of samplers typically used in cosmological applications. Widely used examples of MCMC methods in cosmology include the Metropolis-Hastings and affine ensemble algorithms (Lewis & Bridle 2002; Lewis 2013; Goodman & Weare 2010; Foreman-Mackey et al. 2013), whereas the most widely adopted nested sampling algorithms are multimodal nested sampling and slice-based nested sampling (Feroz & Hobson 2008; Feroz et al. 2009, 2019; Handley et al. 2015a,b).

MCMC and nested sampling methods can struggle to explore large parameter spaces, due to their inherent rejection sampling nature. In these challenging inference scenarios it is useful to resort to gradient-based algorithms, which manage to concentrate the sampling in regions of high posterior density despite the large number of model parameters. A popular gradient-based method is Hamiltonian Monte Carlo (HMC, Duane et al. 1987; Neal 1996), which formulates the problem of sampling the posterior distribution as the dynamical evolution of a particle with position  $\boldsymbol{\theta}$  and momentum  $\mathbf{p}$ . The Hamiltonian of the system is written as:

$$\mathcal{H}(\boldsymbol{\theta}, \mathbf{p}) = \frac{1}{2} \mathbf{p}^T \mathcal{M}^{-1} \mathbf{p} + \mathbf{U}(\boldsymbol{\theta}), \quad (3)$$

where  $\mathcal{M}$  is a “mass matrix”, which is assumed to be the covariance matrix of a zero-mean multivariate Gaussian distribution used to sample  $\mathbf{p}$ , and the potential energy  $\mathbf{U}(\boldsymbol{\theta})$  is defined as:

$$\mathbf{U}(\boldsymbol{\theta}) \equiv -\ln p(\boldsymbol{\theta}|\mathbf{d}). \quad (4)$$

Starting from an initial point in the phase space  $(\boldsymbol{\theta}, \mathbf{p})$ , it is possible to collect samples of the posterior distribution by numerically solving the Hamilton's equations using a leapfrog algorithm. A new proposed state  $(\boldsymbol{\theta}^*, \mathbf{p}^*)$  is then either accepted or rejected based on the new energy value  $\mathcal{H}(\boldsymbol{\theta}^*, \mathbf{p}^*)$ . HMC can thus be seen as a modification to the

original Metropolis-Hastings algorithm, which leverages the analogy with a Hamiltonian system to find a better proposal distribution and results in a higher acceptance rate.

A practical difficulty of HMC is the need for tuning of the hyperparameters governing the leapfrog numerical integration of the Hamiltonian dynamics. These are the number and the size of steps to be taken by the integrator before the sampler changes direction to a new random one. These numbers can be particularly hard to tune and lead to inefficient sampling of the posterior. The No U-Turn Sampler (NUTS, Hoffman & Gelman 2014) tackles this issue by forcing the sampler to avoid U-turns in parameter space. In particular, rather than fixing the number of integration steps, NUTS adjusts the integration length by running the leapfrog algorithm until the trajectory starts to return to previously-visited regions of the parameter space; while the number of model evaluations increases, this leads to a higher acceptance rate, and therefore to faster and more reliable convergence.

In our experiments, we use the NUTS implementation provided by the `NumPyro` library (Bingham et al. 2019; Phan et al. 2019). We set the integration step size to  $10^{-3}$ , and find no difference in the final results by increasing or decreasing this value by one order of magnitude. Additionally, we set the maximum number of model evaluations before sampling a new momentum to  $2^7$ , and specify a block mass matrix according to the expected correlations among parameters. Finally, to further improve the geometry of the problem we perform a reparameterisation of the inference variables: all of the parameters with a Gaussian prior distribution are decentered (Gorinova et al. 2020), while all of those with a uniform prior are rescaled to  $\mathcal{U}[-5, 5]$ . All original prior distributions are reported in Table 1.

We run the NUTS algorithm on three NVIDIA A100 GPUs with 80 GB of memory. Using multiple GPUs allows us to showcase the `pmap` feature of JAX to distribute the NUTS chains over multiple GPU devices. We report below an example snippet to run inference over multiple GPUs using `NumPyro`, where the parallelisation happens simultaneously over a single device and across multiple devices.

```
def do_mcmc(rng_key, n_vectorized=8):
    # All posterior details are defined in this kernel
    nuts_kernel = NUTS(log_posterior)
    mcmc = MCMC(
        nuts_kernel,
        num_chains=n_vectorized,
        chain_method="vectorized"
    )
    mcmc.run(rng_key)
    return {**mcmc.get_samples()}

# Number of devices to pmap over
n_parallel = jax.local_device_count()
rng_ks = jax.random.split(PRNGKey(rng_seed), n_parallel)
samples = pmap(do_mcmc)(rng_ks)
```

In this example, 8 chains are run on each GPU, and the total number of GPUs available is determined at run time.

### 2.4. Likelihoods

To test the computational efficiency and accuracy of our `CosmoPower-JAX` emulators, we run examples of cosmological inference on large parameter spaces, such as

Parameter	Prior range	Fiducial value
Cosmology	$\omega_b = \Omega_b h^2$	$\mathcal{U}[0.01875, 0.02625]$
	$\omega_{\text{cdm}} = \Omega_{\text{cdm}} h^2$	$\mathcal{U}[0.05, 0.255]$
	$h$	$\mathcal{U}[0.64, 0.82]$
	$n_s$	$\mathcal{U}[0.84, 1.1]$
$\ln 10^{10} A_s$	$\mathcal{U}[1.61, 3.91]$	3.047
Baryons	$c_{\min}$	$\mathcal{U}[2, 4]$
	$\eta_0$	$\mathcal{U}[0.5, 1]$
Nuisance S1	$A_{\text{IA},i}^{\text{S1}}$	$i = 1, \dots, 10$
	$D_{z_i, \text{source}}^{\text{S1}}$	$i = 1, \dots, 10$
	$m_i^{\text{S1}}$	$i = 1, \dots, 10$
	$D_{z_i, \text{lens}}^{\text{S1}}$	$i = 1, \dots, 10$
	$b_i^{\text{S1}}$	$i = 1, \dots, 10$
Nuisance S2	$A_{\text{IA},i}^{\text{S2}}$	$i = 1, \dots, 10$
	$D_{z_i, \text{source}}^{\text{S2}}$	$i = 1, \dots, 10$
	$m_i^{\text{S2}}$	$i = 1, \dots, 10$
	$D_{z_i, \text{lens}}^{\text{S2}}$	$i = 1, \dots, 10$
	$b_i^{\text{S2}}$	$i = 1, \dots, 10$
Nuisance S3	$A_{\text{IA},i}^{\text{S3}}$	$i = 1, \dots, 10$
	$D_{z_i, \text{source}}^{\text{S3}}$	$i = 1, \dots, 10$
	$m_i^{\text{S3}}$	$i = 1, \dots, 10$
	$D_{z_i, \text{lens}}^{\text{S3}}$	$i = 1, \dots, 10$
	$b_i^{\text{S3}}$	$i = 1, \dots, 10$

**Table 1:** Prior distributions and fiducial values of the cosmological and nuisance parameters for the simulated analyses performed in this work. Uniform (Gaussian) prior distributions are indicated with  $\mathcal{U}$  ( $\mathcal{N}$ ). For the cosmological parameters and the baryonic feedback parameters ( $c_{\min}, \eta_0$ ) the prior range corresponds to the range of validity of our emulators. The superscripts S1, S2 and S3 refer to three simulated Stage IV surveys, whose details we discuss in Sect. 2.4.

those that will characterise the analysis of future surveys. We consider a power spectrum analysis of both cosmic shear alone, as well as in cross-correlation with galaxy clustering (3x2pt), which in recent years has become the standard method to combine information on the cosmic shear and galaxy clustering field (e.g. [Joachimi & Bridle 2010](#); [Sanchez et al. 2021](#); [Heymans et al. 2021](#); [Abbott et al. 2022](#)). Redshift information is included in the analysis through tomography, assigning galaxies to one of  $N_{\text{bins}}$  bins based on their photometric redshift. The angular power spectra of the probes are jointly modelled computing all of the unique correlations between tomographic bins  $i, j = 1, \dots, N_{\text{bins}}$ . In the following we briefly review the modelling of the power spectra for cosmic shear, galaxy clustering and their cross-correlation

	S1	S2	S3
$f_{\text{sky}}$	0.35	0.05	0.45
$\bar{n}_{\text{source}}$ [gal/arcmin $^2$ ]	30	50	50
$\bar{n}_{\text{lens}}$ [gal/arcmin $^2$ ]	40	55	60
$\sigma_{\epsilon}$	0.30	0.25	0.35

**Table 2:** Specifications for the three Stage IV surveys S1, S2 and S3 that we consider in this work. All details can be found in Sect. 2.4.

(“galaxy-galaxy lensing”), as well as describe the Stage IV surveys we take into consideration. We follow the notation of SM22.

Angular power spectra for the three probes can be expressed as integrals of the matter power spectrum  $P_{\delta\delta}(k, z)$  (a function of wavevector  $k$  and redshift  $z$ ), weighted by pairs of window functions  $W$  for the shear ( $\gamma$ ), clustering (n) and intrinsic alignment (I) fields:

$$C_{ij}^{AB}(\ell) = \int_0^{\chi_H} d\chi \frac{W_i^A W_j^B}{\chi^2} P_{\delta\delta} \left( k = \frac{\ell + 1/2}{\chi}, z \right), \quad (5)$$

where  $\{A, B\} = \{\gamma, n, I\}$ ,  $\chi$  is the comoving distance (itself a function of redshift), and the upper limit of integration is the Hubble radius  $\chi_H = c/H_0$ , with  $c$  the speed of light and  $H_0$  the Hubble constant. In Eq. (5) we assumed the extended Limber approximation ([LoVerde & Afshordi 2008](#)) which connects Fourier scales  $k$  with angular multipoles  $\ell$ .

The angular power spectrum  $C_{ij}^{\epsilon\epsilon}(\ell)$  of the cosmic shear signal for tomographic bins  $i$  and  $j$  is a combination of a pure shear contribution and an intrinsic alignment contamination:

$$C_{ij}^{\epsilon\epsilon}(\ell) = C_{ij}^{\gamma\gamma}(\ell) + C_{ij}^{I\gamma}(\ell) + C_{ij}^{I\gamma}(\ell) + C_{ij}^{II}(\ell). \quad (6)$$

For a tomographic redshift bin distribution  $n_{i,\text{source}}(z), i = 1, \dots, N_{\text{bins}}$ , the weighting function  $W_i^\gamma(\chi)$  for the cosmic shear field  $\gamma$  is given by:

$$W_i^\gamma(\chi) = \frac{3 H_0^2 \Omega_m}{2 c^2} \frac{\chi}{a} \int_\chi^{\chi_H} d\chi' n_{i,\text{source}}(\chi') \frac{\chi' - \chi}{\chi'}, \quad (7)$$

where  $\Omega_m$  is the matter density parameter and  $a$  is the scale factor. To model the window function for the intrinsic alignment field I, we start from the commonly-used non-linear alignment model ([Hirata & Seljak 2004](#); [Joachimi et al. 2011](#)):

$$W_i^I(\chi) = -A_{\text{IA}} \left( \frac{1+z}{1+z_p} \right)^{\eta_{\text{IA}}} \frac{C_1 \rho_{\text{cr}} \Omega_m}{D(\chi)} n_{i,\text{source}}(\chi), \quad (8)$$

with two free parameters  $A_{\text{IA}}$  and  $\eta_{\text{IA}}$ ; the linear growth factor  $D(\chi)$ , the critical matter density  $\rho_{\text{cr}}$ , a constant  $C_1$  and a pivot redshift  $z_p$  also enter Eq. (8). We modify the redshift dependence in Eq. (8) by setting  $\eta_{\text{IA}} = 0$  and using one amplitude parameter  $A_{\text{IA},i}$  for each redshift bin  $i$ . This gives more flexibility to the modelling, at the cost of increasing the number of free parameters. Thus, the

window function for the intrinsic alignment field reads:

$$W_i^I(\chi) = -A_{IA,i} \frac{C_1 \rho_{cr} \Omega_m}{D(\chi)} n_{i,\text{source}}(\chi). \quad (9)$$

We include a multiplicative bias in our modelling of the cosmic shear signal. This keeps into account that the ellipticities measured in a survey are typically biased with respect to an ideal measurement, due to e.g. point spread function modelling errors, selection biases or detector effects (Huterer et al. 2006; Amara & Réfrégier 2008; Kitching et al. 2015; Mandelbaum et al. 2018; Taylor & Kitching 2018; Mahony et al. 2022; Cragg et al. 2022). We consider a multiplicative bias coefficient  $m_i$  for each redshift bin  $i$ ; therefore, the multiplicative bias rescales the cosmic shear power spectrum  $C_{ij}^{\epsilon\epsilon}(\ell)$  by a factor  $(1 + m_i)(1 + m_j)$ . Another important source of uncertainty is the imperfect knowledge of the redshift distributions  $n_{i,\text{source}}(z)$ . Errors in these distributions have traditionally been modelled through the addition of a shift parameter  $D_{z_i,\text{source}}$  for each redshift bin  $i$ , which changes the mean of the bin redshift distribution by shifting the distribution  $n_{i,\text{source}}(z)$  to  $n'_{i,\text{source}}(z) = n_{i,\text{source}}(z - D_{z_i,\text{source}})$  (see e.g. Eifler et al. 2021).

For the modelling of the galaxy clustering power spectrum  $C_{ij}^{nn}(\ell)$  we assume a linear bias model between galaxy and dark matter density, with a free parameter  $b_i$  for each redshift bin  $i$ . The window function  $W_i^n$  for the galaxy clustering field  $n$  is then given by:

$$W_i^n(\chi) = b_i n_{i,\text{lens}}(\chi), \quad (10)$$

where for the galaxy clustering we use a different sample of redshift distributions  $n_{i,\text{lens}}(\chi)$ , which is also not perfectly known and therefore includes a set of shifts  $D_{z_i,\text{lens}}$ . We do not take into account redshift space distortions. Finally, the galaxy-galaxy lensing power spectrum is given by

$$C_{ij}^{n\epsilon}(\ell) = C_{ij}^{n\gamma}(\ell) + C_{ij}^{nI}(\ell). \quad (11)$$

The first experiment we run is a simulated cosmic shear analysis of a Stage IV survey (dubbed “S1”). We assume 10 tomographic bins for  $n_{\text{source}}(z)$ , with galaxies following the distribution:

$$n(z) \propto z^2 \exp\left(-(z/z_0)^{1.5}\right). \quad (12)$$

with  $z_0 = 0.64$  (Smail et al. 1994; Joachimi & Bridle 2010). We consider a Gaussian covariance matrix (e.g. Tutusaus et al. 2020) with a sky fraction  $f_{\text{sky}} = 0.35$ , a surface density of galaxies  $\bar{n}_{\text{source}} = 30$  galaxies per arcmin<sup>2</sup>, and an observed ellipticity dispersion  $\sigma_\epsilon = 0.3$ . The  $C(\ell)$  spectra are computed for 30 bin values between  $\ell_{\text{min}} = 30$  and  $\ell_{\text{max}} = 3000$ .

We use the nested sampler `PolyChord` to sample the posterior distribution and run the inference pipeline within `Cobaya` (Lewis 2013). To compute the theoretical predictions for the cosmological observables we use the Core Cosmology Library (CCL, Chisari et al. 2019). The three upper blocks of Table 1 summarise the prior distributions assumed for the parameters used in this analysis. These include:

- five standard  $\Lambda$ CDM cosmological parameters, namely the baryon density  $\omega_b = \Omega_b h^2$ , the cold dark matter density  $\omega_{\text{cdm}} = \Omega_{\text{cdm}} h^2$ , the Hubble parameter  $h$ , the scalar spectral index  $n_s$ , and the primordial power spectrum amplitude  $\ln 10^{10} A_s$ ;
- the `HMcode` parameters  $c_{\text{min}}$ ,  $\eta_0$ ;
- one intrinsic alignment amplitude  $A_{\text{IA}}$  for each of the ten redshift bins;
- one shift parameter  $D_{z,\text{source}}$  for each of the ten source redshift distributions;
- one multiplicative bias coefficient  $m$  for each of the ten redshift bins,

for a total of 37 model parameters.

We run a second experiment in which we consider the joint analysis of three surveys, dubbed “S1”, “S2” and “S3”, each one performing a 3x2pt analysis over 10 redshift bins over different  $z$  ranges.  $n_{\text{source}}(z)$  and  $n_{\text{lens}}(z)$  are sampled from Eq. (12), with different galaxy densities  $\bar{n}_{\text{source}}$  and  $\bar{n}_{\text{lens}}$  reported in Table 2. In this analysis, the cosmological and baryon parameters are unique, while each survey has its own set of nuisance parameters to model redshift distribution shifts, multiplicative biases and galaxy bias. With respect to the cosmic shear analysis, for each survey we add:

- one shift parameter  $D_{z,\text{lens}}$  for each of the ten lens redshift distributions;
- one linear galaxy bias coefficient  $b$  for each of the ten redshift bins,

for a total of 157 parameters. The prior distributions and fiducial values of the nuisance parameters for all surveys are reported in Table 1, while we report all survey specifications in Table 2.

### 3. RESULTS

#### 3.1. Emulator accuracy

Having used the same dataset and training settings, the accuracy of our JAX emulators is in excellent agreement with the results presented in SM22, i.e. the difference with respect to the CAMB test spectra is always sub-percent for both the matter power spectrum and the CMB probes. We do not show the accuracy plots here for brevity, and refer the reader to SM22 for an extended comparison.

In Fig. 1 we then compare the derivatives of the linear matter power spectrum and the non-linear boost with respect to cosmological parameters, using CAMB and finite differences with a five-point stencil as a benchmark. These numerical derivatives rely on a simple Taylor expansion of the function  $f(x)$  being considered, and are calculated as:

$$f'(x) \simeq \frac{-f(x+2s) + 8f(x+s) - 8f(x-s) + f(x-2s)}{12s}, \quad (13)$$

where  $s$  is a small step size. We choose the step size for each derivative by ensuring that the numerical derivative would only change at the sub-percent level, or within

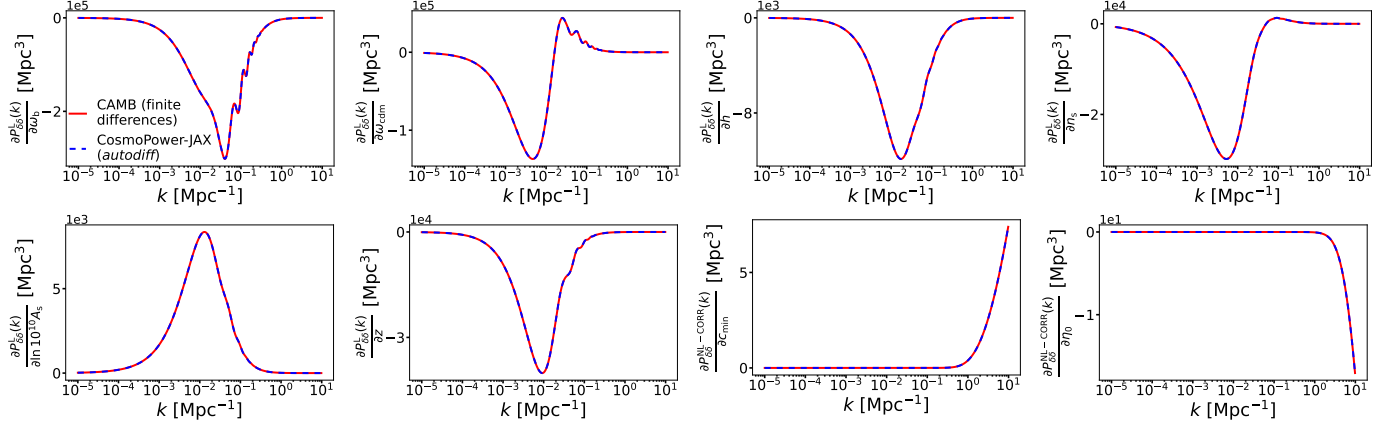


**Figure 1.** Derivatives of the matter power spectrum components as defined in Eq. (1) with respect to cosmological parameters for random samples in the test set. Solid red lines represent finite differences calculated using CAMB and a five-point stencil as in Eq. (13), while dashed blue lines are obtained with the `CosmoPower-JAX` emulator and automatic differentiation (*autodiff*).

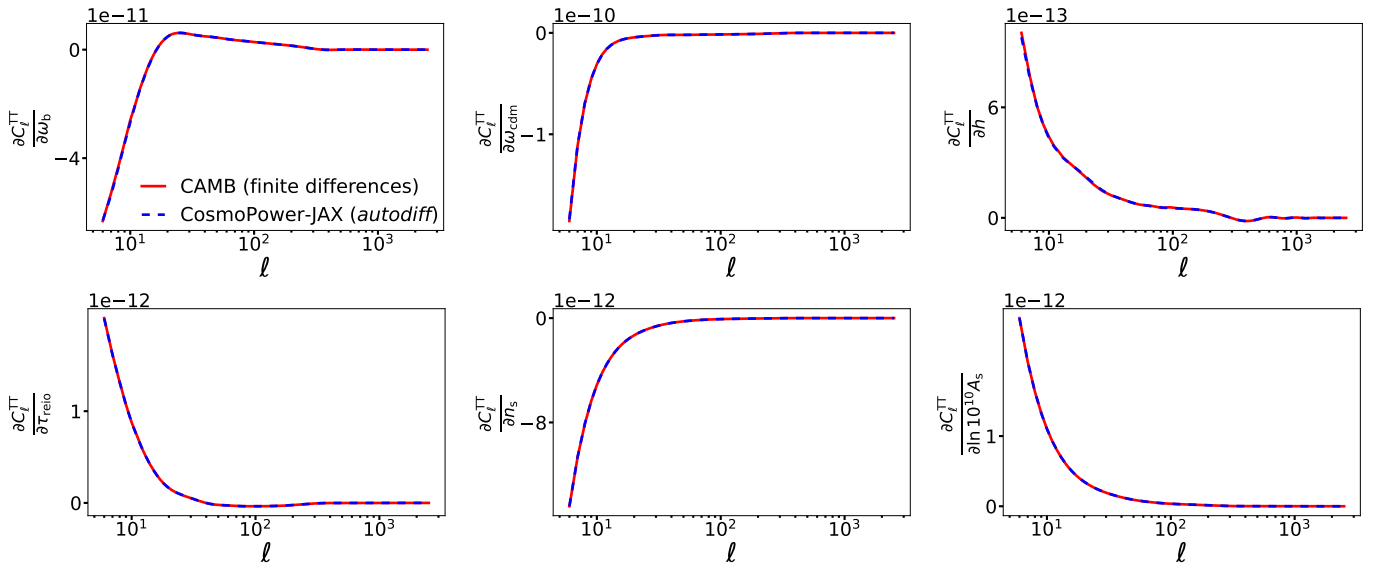


**Figure 2.** Same as in Fig. 1 for the CMB temperature power spectrum  $C_\ell^{\text{TT}}$ .

machine precision, when increasing or decreasing  $s$  by one order of magnitude.

The derivatives computed by our JAX emulators are efficient to obtain and show excellent agreement with the numerical ones, despite the latter being prone to numerical instabilities due to the choice of the step size. Analogously, in Fig. 2 we repeat this comparison for the  $C_\ell^{\text{TT}}$  power spectrum, showing again good agreement for all cosmological parameters.

### 3.2. Bayesian inference

Here we present and comment on the results of running our gradient-based inference pipelines. We emphasise that, while the survey configurations that we consider are representative of the ones expected from upcoming surveys, our goal is not to obtain official forecast predictions, but rather to focus on the challenge represented by the large parameter space required by these analyses, and how to implement viable solutions to efficiently explore these spaces.

In Fig. 3 we show the posterior contours for the cosmo-

logical and nuisance parameters in the case of a cosmic shear analysis of a single Stage IV-like survey. The results obtained with NUTS and the `CosmoPower-JAX` emulators on three GPUs in one day are in excellent agreement with those yielded by the `PolyChord` sampler using CAMB and CCL, which however require about 4 months on 48 2.60 GHz Intel Xeon Platinum 8358 CPU cores. The total speed-up factor is then  $\mathcal{O}(10^3)$  in terms of CPU/GPU hours, and  $\mathcal{O}(10^2)$  in terms of actual elapsed time.

In Fig. 4 and Fig. 5 we then show the posterior contours for the 7 cosmological parameters and the 150 nuisance parameters, respectively, of the joint analysis of the three Stage IV-like surveys described in Sect. 2.4. Obtaining the corresponding contours using `PolyChord` and CAMB would be extremely computationally expensive: optimistically, assuming a linear (rather than exponential, see e.g. [Bishop 1995](#)) scaling of the run time with the number of inference parameters, we would expect to be able to obtain such contours in at least 6 years on 48 CPU cores. Therefore, we only show the results with

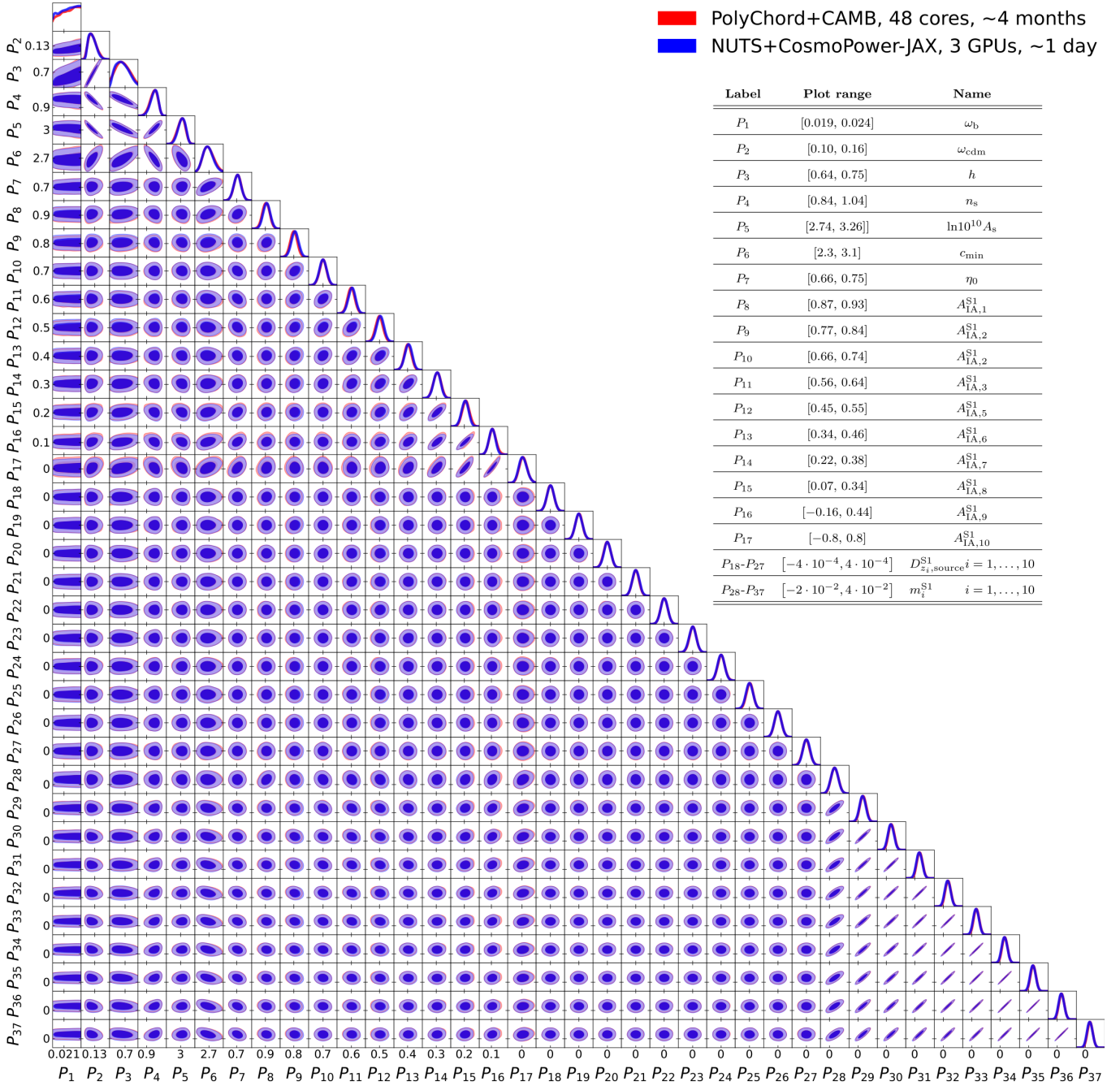


**Figure 3.** Inference results for the cosmic shear analysis of a simulated Stage IV survey with a total of 37 parameters. The contours show the 68% and 95% credibility contours and 1-D marginals for all of the parameters. The inset table reports the plot range and corresponding parameter name of every axis symbol; all parameters are described in Sect. 2.4, while in Table 1 we report the prior distributions and fiducial values. The contours in blue are obtained with the No U-Turn Sampler (NUTS) combined with our CosmoPower-JAX emulators. The contours in red are produced using the PolyChord sampler together with the Boltzmann code CAMB. The CosmoPower-JAX results are obtained over 3 graphics processing units (GPUs) in about 1 day, while the benchmark ran on 48 CPU cores for about 4 months, so that the total speed-up factor in terms of CPU/GPU hours is  $\mathcal{O}(10^3)$ . All of the contours shown in this paper are plotted using GetDist (Lewis 2019).

NUTS and **CosmoPower-JAX**, which we obtain in about 3 days over 3 GPUs, for a total speed-up factor of  $\mathcal{O}(10^4)$  in terms of CPU/GPU hours. These results are unbiased and in good agreement with the fiducial values of our analysis.

#### 4. CONCLUSIONS

We presented **CosmoPower-JAX**, a JAX-based implementation of the cosmological neural emulator **CosmoPower** (Spurio Mancini et al. 2022). **CosmoPower-JAX** adopts the same emulation methods of the original TensorFlow-based version of **CosmoPower**, but implements them using the JAX library. The key feature of JAX is the ability to automatically differentiate functions written in common Python libraries, such as NumPy. Additionally, JAX allows NumPy software to be dynamically compiled, evaluated in batch, and run on graphics processing units (GPUs) and tensor processing units (TPUs). In this paper, we made use of these JAX features to show how they can accelerate Bayesian cosmological inference by orders of magnitude.

We started by training a set of **CosmoPower-JAX** emulators of matter and cosmic microwave background (CMB) power spectra, using the same datasets of Spurio Mancini et al. (2022). We compared the accuracy of our JAX-based emulators with the Boltzmann code CAMB, showing excellent agreement both at the power spectra level as well as at the level of their derivatives.

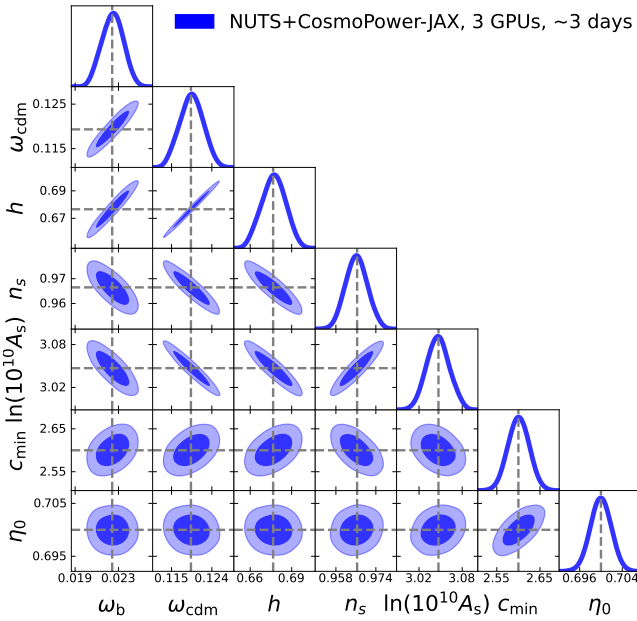


**Figure 4.** Inference results for the joint analysis of three simulated Stage IV surveys, each performing a 3x2pt analysis, for a total of 157 model parameters. Here we show the posterior contours for the cosmological parameters, while we report the marginal distribution of the nuisance parameters in Fig. 5. The blue contours represent the 68% and 95% credibility contours and 1-D marginals. These are obtained with the No U-Turn Sampler (NUTS) combined with our **CosmoPower-JAX** emulators in about 3 days on 3 graphics processing units (GPUs). Dashed grey lines represent the fiducial values, reported in Table 1 together with the prior distributions.

Crucially, rather than being obtained with finite differences, which are prone to numerical instabilities and require fine-tuning of the step size, derivatives of the power spectra with **CosmoPower-JAX** are obtained straightforwardly and efficiently with the built-in automatic differentiation (*autodiff*) features provided by JAX. We note that the usefulness of our differentiable power spectra emulators is not limited to 2-point-statistics analyses of cosmological fields: for example, field-level inference pipelines (e.g. Makinen et al. 2021, 2022; Loureiro et al. 2023; Porqueres et al. 2023) greatly benefit from efficient access to power spectra and their gradients.

We combined our emulators with the JAX-based cosmological library **jax-cosmo** (Campagne et al. 2023) to write likelihood functions that are fully differentiable by virtue of their pure-JAX implementation. Running these likelihoods within inference pipelines using gradient-based Monte Carlo algorithms like the No U-Turn Sampler (NUTS), we showed how to use **CosmoPower-JAX** to perform cosmological Bayesian inference over parameter spaces with  $\mathcal{O}(100)$  parameters, using multiple graphics processing units (GPUs) in parallel. We performed a cosmic shear analysis for a Stage IV-like survey configuration with a total of 37 parameters, showing good agreement with standard nested sampling inference performed with CAMB, while being  $\mathcal{O}(10^3)$  times faster. We finally showed that with **CosmoPower-JAX** and NUTS it is possible to perform a combined Bayesian inference on three different Stage IV-like surveys, each performing a joint cosmic shear and galaxy clustering analysis (3x2pt), for a total of 157 parameters, of which 150 represent nuisance parameters used to model systematic effects for each survey. We obtained unbiased posterior contours in about 3 days on 3 GPUs, as opposed to an optimistic estimate of at least 6 years needed to obtain the same results with traditional sampling methods and standard Boltzmann codes, for a total speed-up factor of  $\mathcal{O}(10^4)$  in terms of CPU/GPU hours.

Developing fully differentiable, GPU-accelerated implementations of key analysis pipelines is of the utmost importance to tackle the massive computational requirements imposed by upcoming Stage IV surveys. To this purpose, we envision the use of differentiable libraries such as TensorFlow, JAX and PyTorch to become standard practice in cosmological software implementations, not least because they can all be used within the Python programming language, which is becoming the de facto standard programming language in both the cosmological and machine learning communities.

Libraries such as **CosmoPower-JAX** and **jax-cosmo** are therefore of paramount importance for the success of next generation surveys. To this purpose, we plan to integrate the public release of **CosmoPower-JAX** with the **jax-cosmo** library. In parallel, we will explore improved gradient-based posterior samplers, such as those described in Ver Steeg & Galstyan (2021); Park (2021); Robnik et al. (2022); Karamanis et al. (2022); Wong et al. (2023), to further improve the sampling efficiency, and thus the usefulness of our differentiable emulators.

#### ACKNOWLEDGEMENTS

We are grateful to Erminia Calabrese, Benjamin Joachimi and Jason McEwen for useful discussions and feedback on this work. DP was supported by a Swiss Na-

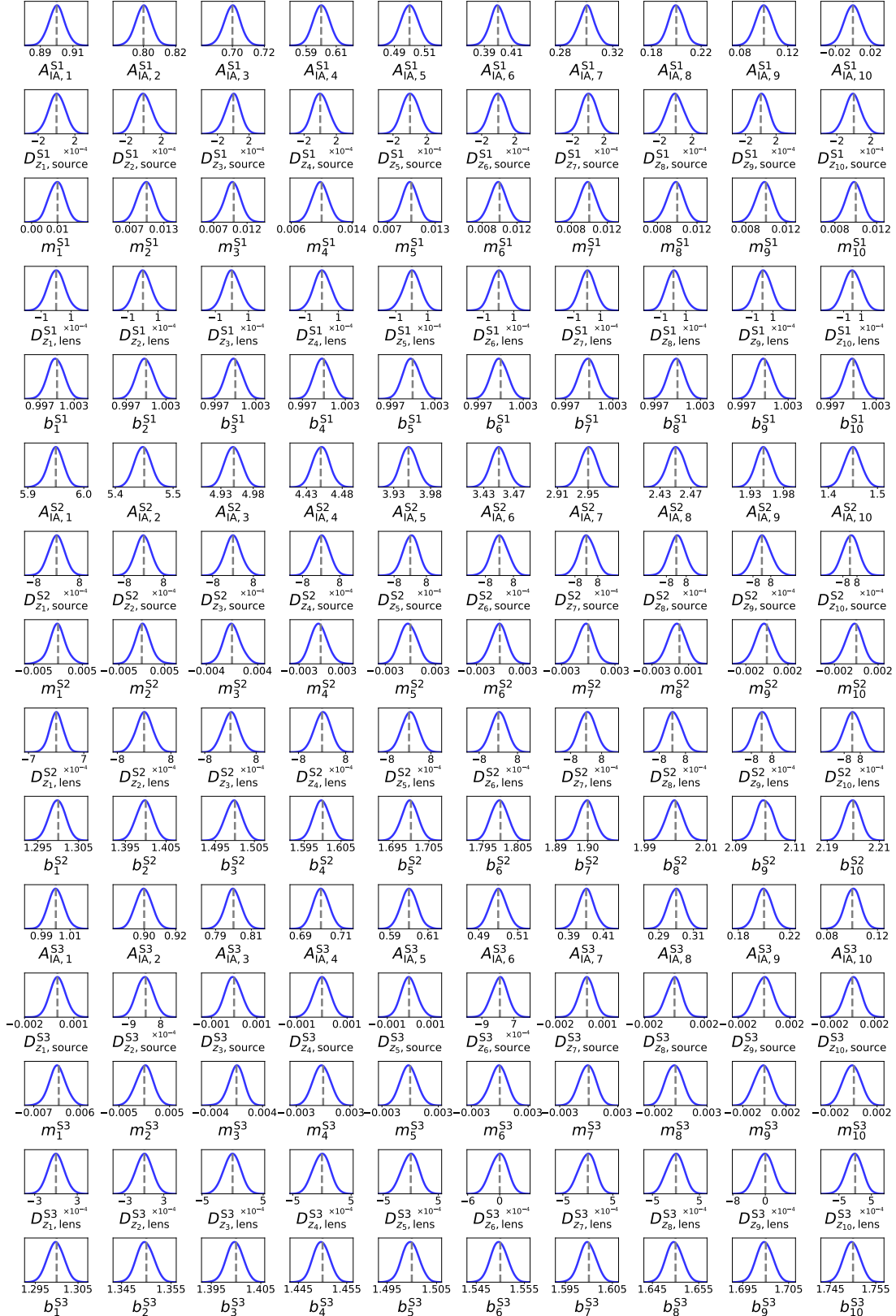


**Figure 5.** Marginal posterior distributions obtained in about 3 days on 3 graphics processing units (GPUs) with our CosmoPower-JAX emulators and the No U-Turn Sampler (NUTS) for the nuisance parameters of the the joint analysis of three simulated Stage IV surveys. Each survey performs a 3x2pt analysis, for a total of 157 parameters. The corresponding cosmological constraints can be found in Fig. 4. Dashed grey lines represent the fiducial values, reported in Table 1 together with the prior distributions.

tional Science Foundation (SNSF) Professorship grant (No. 202671). ASM acknowledges support from the MSSL STFC Consolidated Grant ST/W001136/1. Part of the computations were performed on the Baobab cluster at the University of Geneva. This work has been partially enabled by funding from the UCL Cosmoparticle Initiative. The authors are pleased to acknowledge that part of the work reported on in this paper was performed using the Princeton Research Computing resources at Princeton University which is a consortium of groups led by the Princeton Institute for Computational Science and Engineering (PICSciE) and Office of Information Technology's Research Computing.

#### DATA AVAILABILITY

We make the `CosmoPower-JAX` emulators available in this GitHub repository (<https://github.com/dpiras/cosmopower-jax>, also accessible by clicking the icon .

#### REFERENCES

Abadi M., et al., 2015, TensorFlow: Large-Scale Machine Learning on Heterogeneous Systems, <https://www.tensorflow.org/>

Abazajian K. N., et al., 2016, arXiv e-prints, p. arXiv:1610.02743

Abbott T. M. C., et al., 2022, *Phys. Rev. D*, **105**, 023520

Ade P., et al., 2019, *Journal of Cosmology and Astroparticle Physics*, **2019**, 056–056

Amara A., Réfrégier A., 2008, *Monthly Notices of the Royal Astronomical Society*, **391**, 228

Aricò G., Angulo R., Zennaro M., 2022, *Open Research Europe*, **1**

Audren B., Lesgourgues J., Benabed K., Prunet S., 2013, *JCAP*, **1302**, 001

Balkenhol L., et al., 2022, arXiv e-prints, p. arXiv:2212.05642

Bartholomew-Biggs M., Brown S., Christianson B., Dixon L., 2000, *Journal of Computational and Applied Mathematics*, **124**, 171

Baydin A. G., Pearlmutter B. A., Radul A. A., Siskind J. M., 2018, *Journal of Machine Learning Research*, **18**, 1

Betancourt M., 2017, arXiv e-prints, p. arXiv:1701.02434

Bingham E., et al., 2019, *J. Mach. Learn. Res.*, **20**, 28:1

Bishop C., 1995, *Neural networks for pattern recognition*. Oxford University Press, USA

Blas D., Lesgourgues J., Tram T., 2011, *J. Cosmology Astropart. Phys.*, **2011**, 034

Blei D. M., Kucukelbir A., McAuliffe J. D., 2017, *Journal of the American Statistical Association*, **112**, 859

Bolliet B., Spurio Mancini A., Hill J. C., Madhavacheril M., Jense H. T., Calabrese E., Dunkley J., 2023, arXiv e-prints, p. arXiv:2303.01591

Brinckmann T., Lesgourgues J., 2019, *Physics of the Dark Universe*, **24**, 100260

Brooks S., Gelman A., Jones G., Meng X.-L., eds, 2011, *Handbook of Markov Chain Monte Carlo*. Chapman and Hall/CRC, doi:10.1201/b10905, <https://doi.org/10.1201%2Fb10905>

Burger P. A., et al., 2023, *A&A*, **669**, A69

Campagne J.-E., et al., 2023, arXiv e-prints, p. arXiv:2302.05163

Chisari N. E., et al., 2019, *The Astrophysical Journal Supplement Series*, **242**, 2

Cragg C., Duncan C. A. J., Miller L., Alonso D., 2022, *Monthly Notices of the Royal Astronomical Society*, **518**, 4909

Duane S., Kennedy A., Pendleton B. J., Roweth D., 1987, *Physics Letters B*, **195**, 216

Eifler T., et al., 2021, *Monthly Notices of the Royal Astronomical Society*, **507**, 1514

Feroz F., Hobson M. P., 2008, *Monthly Notices of the Royal Astronomical Society*, **384**, 449

Feroz F., Hobson M. P., Bridges M., 2009, *Monthly Notices of the Royal Astronomical Society*, **398**, 1601

Feroz F., Hobson M. P., Cameron E., Pettitt A. N., 2019, *The Open Journal of Astrophysics*, **2**

Foreman-Mackey D., Hogg D. W., Lang D., Goodman J., 2013, *Publications of the Astronomical Society of the Pacific*, **125**, 306

Frostig R., Johnson M., Leary C., 2018, in SysML (2018). <https://mlsys.org/Conferences/doc/2018/146.pdf>

Gong Z., Halder A., Barreira A., Seitz S., Friedrich O., 2023, arXiv e-prints, p. arXiv:2304.01187

Goodman J., Weare J., 2010, *Communications in Applied Mathematics and Computational Science*, **5**, 65

Gorinova M., Moore D., Hoffman M., 2020, in III H. D., Singh A., eds, *Proceedings of Machine Learning Research* Vol. 119, *Proceedings of the 37th International Conference on Machine Learning*. PMLR, pp 3648–3657, <https://proceedings.mlr.press/v119/gorinova20a.html>

Günther S., Lesgourgues J., Samaras G., Schöneberg N., Stadtmann F., Fidler C., Torrado J., 2022, *Journal of Cosmology and Astroparticle Physics*, **2022**, 035

Hajian A., 2007, *Phys. Rev. D*, **75**, 083525

Handley W. J., Hobson M. P., Lasenby A. N., 2015a, *Monthly Notices of the Royal Astronomical Society: Letters*, **450**, L61

Handley W. J., Hobson M. P., Lasenby A. N., 2015b, *Monthly Notices of the Royal Astronomical Society*, **453**, 4384

Harris C. R., et al., 2020, *Nature*, **585**, 357

Heymans C., et al., 2021, *A&A*, **646**, A140

Hirata C. M., Seljak U., 2004, *Phys. Rev. D*, **70**, 063526

Hoffman M. D., Gelman A., 2014, *J. Mach. Learn. Res.*, **15**, 1593–1623

Hoffman M. D., Blei D. M., Wang C., Paisley J., 2013, *Journal of Machine Learning Research*, **14**, 1303

Huterer D., Takada M., Bernstein G., Jain B., 2006, *Monthly Notices of the Royal Astronomical Society*, **366**, 101

Ivezić Ž., et al., 2019, *ApJ*, **873**, 111

Jasche J., Wandelt B. D., 2013, *Monthly Notices of the Royal Astronomical Society*, **432**, 894

Jasche J., Kitaura F. S., Li C., Enßlin T. A., 2010, *Monthly Notices of the Royal Astronomical Society*, **409**, 355

Joachimi B., Bridle S. L., 2010, *A&A*, **523**, A1

Joachimi B., Mandelbaum R., Abdalla F. B., Bridle S. L., 2011, *A&A*, **527**, A26

Karamanis M., Nabergoj D., Beutler F., Peacock J. A., Seljak U., 2022, *Journal of Open Source Software*, **7**, 4634

Katafygiotis L., Zuev K., 2008, *Probabilistic Engineering Mechanics*, **23**, 208

Kingma D. P., Ba J., 2015, in Bengio Y., LeCun Y., eds, *3rd International Conference on Learning Representations, ICLR 2015*, San Diego, CA, USA, May 7–9, 2015, Conference Track Proceedings. <http://arxiv.org/abs/1412.6980>

Kitching T. D., Taylor A. N., Cropper M., Hoekstra H., Hood R. K. E., Massey R., Niemi S., 2015, *Monthly Notices of the Royal Astronomical Society*, **455**, 3319

Laureijs R., et al., 2011, arXiv e-prints, p. arXiv:1110.3193

Lavaux G., Jasche J., 2015, *Monthly Notices of the Royal Astronomical Society*, **455**, 3169

Lewis A., 2013, *Phys. Rev. D*, **87**, 103529

Lewis A., 2019, arXiv e-prints, p. arXiv:1910.13970

Lewis A., Bridle S., 2002, *Phys. Rev. D*, **66**, 103511

Lewis A., Challinor A., 2011, CAMB: Code for Anisotropies in the Microwave Background, *Astrophysics Source Code Library*, record ascl:1102.026 (ascl:1102.026)

Liu J., 2009, *Monte Carlo Strategies in Scientific Computing*. Springer, doi:10.1007/978-0-387-76371-2

LoVerde M., Afshordi N., 2008, *Physical Review D*, **78**

Loureiro A., Whiteway L., Sellentin E., Silva Lafaurie J., Jaffe A. H., Heavens A. F., 2023, *The Open Journal of Astrophysics*, **6**, 6

Mahony C., Fortuna M. C., Joachimi B., Korn A., Hoekstra H., Schmidt S. J., Collaboration L. D. E. S., 2022, *Monthly Notices of the Royal Astronomical Society*, **513**, 1210

Makinen T. L., Charnock T., Alsing J., Wandelt B. D., 2021, *Journal of Cosmology and Astroparticle Physics*, **2021**, 049

Makinen T. L., Charnock T., Lemos P., Porqueres N., Heavens A. F., Wandelt B. D., 2022, *The Open Journal of Astrophysics*, **5**

Mandelbaum R., et al., 2018, *Monthly Notices of the Royal Astronomical Society*, **481**, 3170

Margossian C. C., 2019, *WIREs Data Mining and Knowledge Discovery*, **9**, e1305

Mead A. J., Peacock J. A., Heymans C., Joudaki S., Heavens A. F., 2015, *Monthly Notices of the Royal Astronomical Society*, 454, 1958

Mead A. J., Heymans C., Lombriser L., Peacock J. A., Steele O. I., Winther H. A., 2016, *Monthly Notices of the Royal Astronomical Society*, 459, 1468

Mootoovaloo A., Heavens A. F., Jaffe A. H., Leclercq F., 2020, *Monthly Notices of the Royal Astronomical Society*, 497, 2213

Neal R. M., 1996, Bayesian Learning for Neural Networks, Vol. 118 of Lecture Notes in Statistics. Springer-Verlag

Neal R., 2011, in , Handbook of Markov Chain Monte Carlo. Chapman and Hall/CRC, pp 113–162, doi:10.1201/b10905

Neidinger R. D., 2010, *SIAM Review*, 52, 545

Nygaard A., Brinch Holm E., Hannestad S., Tram T., 2022, arXiv e-prints, p. arXiv:2205.15726

Park J., 2021, arXiv e-prints, p. arXiv:2111.06871

Paszke A., et al., 2017, in NIPS 2017 Workshop on Autodiff. <https://openreview.net/forum?id=BJJsrmfCZ>

Paszke A., et al., 2019, in , Advances in Neural Information Processing Systems 32. Curran Associates, Inc., pp 8024–8035, <http://papers.neurips.cc/paper/9015-pytorch-an-imperative-style-high-performance-deep-learning-library.pdf>

Phan D., Pradhan N., Jankowiak M., 2019, arXiv preprint arXiv:1912.11554

Porqueres N., Heavens A., Mortlock D., Lavaux G., Makinen T. L., 2023, arXiv e-prints, p. arXiv:2304.04785

Roberts G. O., Gelman A., Gilks W. R., 1997, *The Annals of Applied Probability*, 7, 110

Robnik J., De Luca G. B., Silverstein E., Seljak U., 2022, arXiv e-prints, p. arXiv:2212.08549

Ruiz-Zapatero J., Hadzhiyska B., Alonso D., Ferreira P. G., García-García C., Mootoovaloo A., 2023, arXiv e-prints, p. arXiv:2301.11978

Sanchez J., Nicola A., Alonso D., Chang C., DESC L., 2021, *Bulletin of the AAS*, 53

Sehgal N., et al., 2019, in *Bulletin of the American Astronomical Society*. p. 6 (arXiv:1906.10134), doi:10.48550/arXiv.1906.10134

Smail I., Ellis R. S., Fitchett M. J., 1994, *Monthly Notices of the Royal Astronomical Society*, 270, 245

Spergel D., et al., 2015, arXiv e-prints, p. arXiv:1503.03757

Spurio Mancini A., Piras D., Alsing J., Joachimi B., Hobson M. P., 2022, *Monthly Notices of the Royal Astronomical Society*, 511, 1771

Spurio Mancini A., Pourtsidou A., 2022, *Monthly Notices of the Royal Astronomical Society: Letters*, 512, L44

Taylor A. N., Kitching T. D., 2018, *Monthly Notices of the Royal Astronomical Society*, 477, 3397

Taylor J. F., Ashdown M. A. J., Hobson M. P., 2008, *Monthly Notices of the Royal Astronomical Society*, 389, 1284

Torrado J., Lewis A., 2021, *Journal of Cosmology and Astroparticle Physics*, 2021, 057

Tutusaus I., et al., 2020, *A&A*, 643, A70

Valade A., Hoffman Y., Libeskind N. I., Graziani R., 2022, *Monthly Notices of the Royal Astronomical Society*, 513, 5148

Ver Steeg G., Galstyan A., 2021, in Advances in Neural Information Processing Systems.

Wong K., Gabrié M., Foreman-Mackey D., 2023, *Journal of Open Source Software*, 8, 5021

Zhang C., Bütepage J., Kjellström H., Mandt S., 2017, *IEEE Transactions on Pattern Analysis and Machine Intelligence*, PP

This paper was built using the Open Journal of Astrophysics L<sup>A</sup>T<sub>E</sub>X template. The OJA is a journal which

provides fast and easy peer review for new papers in the `astro-ph` section of the arXiv, making the reviewing process simpler for authors and referees alike. Learn more at <http://astro.theoj.org>.